SINERGI Vol. 28, No. 3, October 2024: 661-668
http://publikasi.mercubuana.ac.id/index.php/sinergi
http://doi.org/10.22441/sinergi.2024.3.021

Fuzzy logic-based control for robot-guided strawberry harvesting: visual servoing and image segmentation approach

Tresna Dewi[1]*, Muhammad Refo Bambang[1], RD Kusumanto[1], Pola Risma[1], Yurni Oktarina[1], Takahiro Sakuraba[2], Ahmad Fudholi[3], Rusnianasari[4]
[1]Department of Electrical Engineering, Politeknik Negeri Sriwijaya, Indonesia
[2]Department of Creative Engineering, National Institute of Technology Tsuruoka College, Japan.
[3]Solar Energy Research Institute, Universiti Kebangsaan Malaysia, Malaysia,
Research Centre for Electrical Power and Mechatronics LIPI, Indonesia
[4]Department Department of Renewable Energy Engineering, Politeknik Negeri Sriwijaya, Indonesia

Abstract
The concept of digital farming can help farmers increase their agricultural production yield. One of the technologies to support digital farming is robotics, which can be utilized to complete a redundant task efficiently for 24 hours. This paper presents a simple and effective harvesting robot that is applied to harvest a ripe strawberry. The mechanical and electrical design is kept simple to ensure it is reproducible. The input from a proximity sensor and image detection by a Pi camera is utilized by FLC (Fuzzy Logic Controller) to improve the effectiveness of the harvesting task. The image processing method in this study is image segmentation, which fits with the limited source of the microcontroller available in the market. The experiment included 60 times (20 times center, left, and right position) harvesting using the FLC algorithm and 60 times without FLC to show the effectiveness of the proposed method. From 60 experiments without an FLC experiment, there is an 80% hit rate for strawberries positioned in the middle of an image plane and 55% for left and right strawberries. From 60 times of FLC experiment, 95% hit rate for strawberries positioned in the middle of an image plane, 80% for left and right strawberries. The average time required to finish the task without FLC for strawberries in the middle is 13.51 s, the left is 11.04 s, and the right is 17.28 s. While the average time required to finish the task with FLC for strawberry in the middle is 12.90 s, the left side is 11.71 s, and the right side is 10.93 s. This study is intended to show that simple designs can be helpful and affordable when applied to greenhouse farming in Indonesia.

Keywords:
Digital farming;
Fuzzy Logic Controller;
Image Segmentation;
Visual Servoing;

Article History:
Received: January 30, 2024
Revised: March 28, 2024
Accepted: April 7, 2024
Published: October 2, 2024

Corresponding Author:
Tresna Dewi
Electrical Engineering Department, Politeknik Negeri Sriwijaya, Indonesia
Email: tresna_dewi@polsri.ac.id

INTRODUCTION

Located in an equatorial climate, Indonesia benefits from favorable agricultural conditions throughout the year, making agriculture a key driver of economic growth. The adoption of digital farming technologies can address agricultural yield production. Digital farming entails the application of automated systems in agriculture, such as automatic greenhouses [1][2]. This concept can potentially enhance farming efficiency and performance [1, 2, 3, 4, 5, 6, 7, 8].

Robotics applications in agriculture are one of the technologies that can be used to achieve digital farming. Robots can be employed as automatic harvesting devices, and the most suitable robot type is the arm robot manipulator since its arm can be customized to imitate humans [9, 10, 11, 12, 13, 14, 15, 16]. The robotics system

is made possible for farmers due to the lower cost of the components needed to build a robot. A robot used in agriculture does not have to be sophisticated [17]; an arm robot equipped with some sensors (camera and proximity sensors) is sufficient for a harvesting robot. Image processing for target detection is one of the crucial things to be considered. The problem with image processing is that it requires a high computational resource to complete the task [18, 19, 20, 21, 22]; hence, the challenge is designing an image processing system that can fit into the limited memory of current microcontrollers.

Visual servoing controls robot motion by using the feedback from image detection provided by the camera [12, 18, 19, 20]. Image detection provides information on fruit distance and position. The problem is that fruit position is dynamic from plant to plant, and lighting is also a problem in target detection. However, sophisticated methods require longer computational time and more resources, while in this agriculture application, the simple yet effective robot is more desired.

This paper presents a simple and effective harvesting robot that is applied to pick up ripe strawberries using image segmentation for target detection whose computational time fits the limited source of the current microcontroller available in the market. Fuzzy Logic Controller (FLC) is implemented to enhance the efficiency of the proposed method [23, 24, 25, 26, 27]. The kinematics design is also discussed to achieve an ideal robot model. Experiments are conducted to demonstrate the effectiveness of the proposed method, which shows the hit-and-miss of strawberry harvesting. The robot design is presented in this paper to show the affordability and reproducibility of the proposed robot.

METHOD

The harvesting robot prototype proposed in this study implements the method shown in Figure 1. Image segmentation is utilized for object detection, which in this study is the strawberry coordinate position.

As the robot detects the target position, the microcontroller moves the servo motors attached to the base, joints, and end-effector. The servo motion speeds are regulated based on the distance between the end-effector and the target, which is indicated by proximity sensor detection and controlled by FLC.

The robot is moved by six motor servos for the base, joint 1, joint 2, the wrist of the end-effector, the scissor, and the gripper. The scissor and gripper positions are adjusted to imitate the human hand while harvesting fruits.

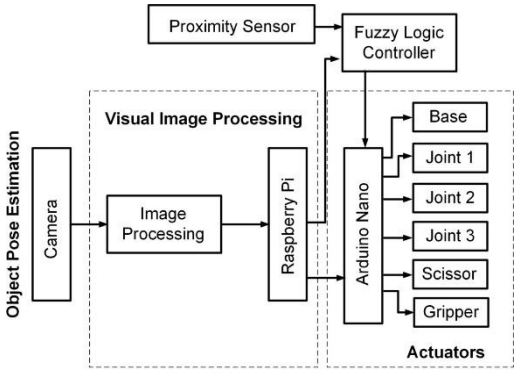

Figure 1. Diagram block of the proposed method

Robot Mechanical and Electrical and Design

The robot considered in this study is a 3DOF arm robot designed to harvest strawberries in a greenhouse setting. The robot design is shown in Figure 2 and Figure 3. The mechanical design is shown in Figure 2a, which shows the servos moving the joints and end-effector.

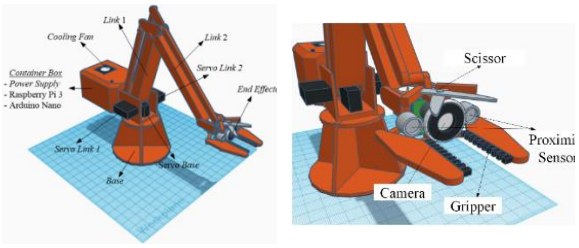

(a) Mechanical (b) End-effector

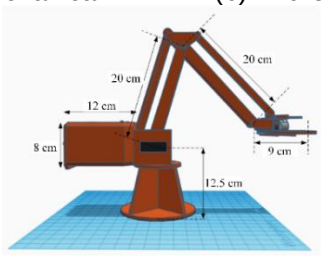

(c) Robot dimension

Figure 2. Robot's mechanical design

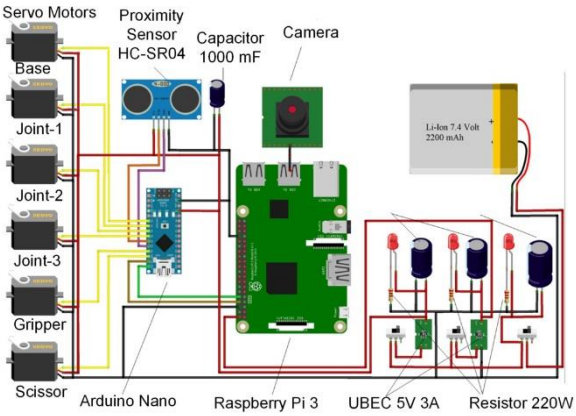

Figure 3. The electrical design of the robot is in Figure 2.

The end-effector consists of a scissor to cut the fruit and a gripper to grab the fruit, and Figure 2b shows the position of the scissor, camera, and gripper. The camera is positioned as the eye in the hand of the robot, which is beneficial to avoid occlusion. Figure 2c shows the robot's dimensions, which are designed based on the size of a strawberry plant, and the electrical connection is shown in Figure 3.

As the target coordinates are located, the robot is moved by the servo motors within a range of 15° to 165° for the base. The second servo is the actuator to move joint 1 within the motion range of 25° to 105°, and the servo for joint 2 within the motion range of 135° to 175°. The joint between link 2 and the end-gripper is designed to move from 135° to 175°. The gripper servo moves within the motion range of 5° to 80°, and the scissor servo is within the motion range of 0° to 180°. The distance of the end-effector to the object is set to be 9 cm.

Robot Kinematics Modeling

Kinematics modeling is the process of modeling the robot by analyzing the robot's motion without considering the force and torque applied to the robot. Kinematics modeling is started by transferring the robot's links and joints in Figure 4 into the Denavit-Hartenberg (DH) Table (Table 1) to find the best parameters for the robot.

The transformation matrix ${}^{3}_{0}T$ is given by ${}^{0}_{1}\mathrm{T}(q_1)$, ${}^{1}_{2}\mathrm{T}(q_2)$, and ${}^{2}_{3}\mathrm{T}(q_3)$, which are resulted to rotation matrices as follow:

$$ {}^{0}_{1}R = \begin{bmatrix} c_1 & 0 & s_1 \\ s_1 & 0 & -c_1 \\ 0 & 1 & 0 \end{bmatrix}, {}^{1}_{2}R = \begin{bmatrix} c_2 & -s_2 & 0 \\ s_2 & c_2 & 0 \\ 0 & 0 & 1 \end{bmatrix}, \text{ and } {}^{2}_{3}R = \begin{bmatrix} c_3 & -s_3 & 0 \\ s_3 & c_3 & 0 \\ 0 & 0 & 1 \end{bmatrix}, \quad (1) $$

where c_1 is $\cos q_1$, s_1 is $\sin q_1$, c_2 is $\cos q_2$, s_2 is $\sin q_2$, c_3 is $\cos q_3$, and s_3 is $\sin q_3$.

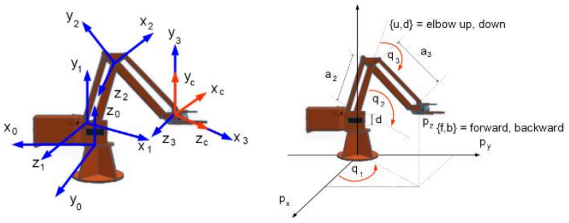

(a) Frames (b) parameters

Figure 4. Arm robot frames for DH Table

Table 1. DH Convention for the robot in Figure 4.

i	α_i	d_i	a_i	θ_i
1	$\frac{\pi}{2}$	d	0	q_1
2	0	0	a_2	q_2
3	0	0	a_3	q_3

Therefore, the position ($\boldsymbol{p} = [\mathrm{p_x} \quad \mathrm{p_y} \quad \mathrm{p_z}]^{\boldsymbol{T}}$) of the origin O_3 of frame 3 is given by

$$ \begin{bmatrix} \boldsymbol{p} \\ 1 \end{bmatrix} = {}^{0}_{1}\mathrm{T}(q_1)\ {}^{1}_{2}\mathrm{T}(q_2){}^{2}_{3}\mathrm{T}(q_3) \begin{bmatrix} 0 \\ 1 \end{bmatrix}, \quad (2) $$

and resulted in

$$ p = \boldsymbol{f}(\boldsymbol{q}) = \begin{bmatrix} c_1(a_2c_2 + a_3c_{23}) \\ s_1(a_2c_2 + a_3c_{23}) \\ d + a_2s_2 + a_3s_{23} \end{bmatrix}, \quad (3) $$

or $\mathrm{p_x}$ is $c_1(a_2c_2 + a_3c_{23})$, $\mathrm{p_y}$ is $s_1(a_2c_2 + a_3c_{23})$, and $\mathrm{p_z}$ is $d + a_2s_2 + a_3s_{23}$.

The inverse kinematics solution is achieved by multiplying both sides from (3) as follows.

$$ p_x^2 + p_y^2 + (p_z - d)^2 = c_1^2(a_2c_2 + a_3c_{23})^2 + s_1^2(a_2c_2 + a_3c_{23})^2 + (a_2s_2 + a_3s_{23})^2, \quad (4) $$

then

$$ \begin{aligned} p_x^2 + p_y^2 + (p_z - d)^2 &= a_2^2 + a_3^2 \\ &\quad + 2a_2a_3(c_2c_{23} + s_2s_{23}) \\ &= a_2^2 + a_3^2 + 2a_2a_3c_3, \end{aligned} \quad (5) $$

and by rearranging (5), yield

$$ c_3 = \frac{(p_x^2+p_y^2+(p_z-d)^2-a_2^2-a_3^2)}{2a_2a_3}, \quad (6) $$

where $c_3 \in (-1,1)$ to ensure the robot is inside its workspace and

$$ s_3 = \pm\sqrt{1 - c_3^2}, \quad (7) $$

in which resulted in $q_3 = atan(s_3, c_3)$ for positive (+) result and $q_3 = atan(-s_3, c_3)$ for negative one.

The base motion generates the angle q_1, and to get real solutions, $p_x^2 + p_y^2 > 0$; otherwise, q_1 is undefined and infinite solutions. Therefore,

$$ c_1 = \frac{p_x}{\pm\sqrt{p_x^2+p_y^2}}, \text{ and } s_1 = \frac{p_y}{\pm\sqrt{p_x^2+p_y^2}}, \quad (8) $$

where two solutions occurs; for positive solution $q_1 = atan2(p_y, p_x)$, and $q_1 = atan2(-p_y, -p_x)$ for negative.

The angle q_2 is solved by considering the elbow's forward, backward, up, and down motion, as shown in Figure 4(b). By rearranging (5) and (6), yields

$$ c_1p_x + s_1p_y = a_2c_2 + a_3c_{23} = (a_2+a_3c_3)c_2 - a_3c_3s_2, \quad (9) $$

and

$$ p_z - d = a_2s_2 + a_3s_{23} = a_3c_3c_2 + (a_2+a_3c_3)s_2. \quad (10) $$

The Jacobian matrix from camera frame ${}^{c}\boldsymbol{J}(\boldsymbol{q})$ gives

$$ \begin{aligned} {}^{c}\boldsymbol{J}(\boldsymbol{q}) &= {}^{0}_{c}R^T\ {}^{0}\boldsymbol{J}(\boldsymbol{q}) = \\ &{}^{3}_{c}R^T\left({}^{2}_{3}R^T(q_3)\left({}^{1}_{2}R^T(q_2)\left({}^{0}_{1}R^T(q_1)\,{}^{0}\boldsymbol{J}(\boldsymbol{q})\right)\right)\right), \\ {}^{c}\boldsymbol{J}(\boldsymbol{q}) &= \begin{bmatrix} a_2c_2 + a_3c_{23} & 0 & 0 \\ 0 & a_3 + a_2c_2 & a_3 \\ 0 & a_2c_2 & 0 \end{bmatrix}, \end{aligned} \quad (11) $$

where the related joint velocity ${}^{c}_{}\boldsymbol{v}$ is given by ${}^{c}_{}\boldsymbol{J}(\boldsymbol{q})\dot{\boldsymbol{q}}$ as the linear velocity of camera frame origin expressed in the camera frame. The linear velocity of the robot's end-effector is ${}^{c}_{}\boldsymbol{v} = {}^{c}_{}\boldsymbol{J}(\boldsymbol{q})\dot{\boldsymbol{q}}$.

Image Segmentation for Target Detection

Image segmentation for visual servoing considered in this study is given in Figure 5. The output is the target position in xy axis, which is conducted online, and the steps are as follows:

1. The camera captures the raw image of the strawberry.
2. The raw image is converted to a grayscale image.
3. The gray image is processed with HSV (Hue, Saturation, Value) given as H = 0, S = 90, and V = 160. The value of H is set to 0 for the reddish color.
4. The masking was conducted by replacing the white a reddish color.

Fuzzy Logic Controller (FLC) Design

FLC design starts by identifying the inputs for fuzzification. FLC is to move the robot to cut and grab the target based on the target detection. The data inputs are achieved from the target detection by image segmentation and distance approximation by the proximity sensor attached to the gripper.

The inputs and output relationship are translated into Rules in Table 2 as the reasoning process and membership functions of inputs and output, where Dect is detection, F is far, N is near, M is medium, Ft is fast, Sl is slow. How far the robot can extend to reach the target is defined by the angles of each joint presented in kinematics analysis, including considering the position of the target, which is defined as the object position in *the x* and *y*-axis. The kinematics analysis also defines the end-effector velocity. The target detection position presented in the rules is only for middle detection; other position rules are not presented to avoid the excessively lengthy table.

Table 2. The rules considered in this study

No	Input		Output			
	Target	d	X	Y	Grip	Scr
1	No Dect	F	Stop	Stop	Off	Off
2	Left-N	F	Left-Sl	Stop	Off	Off
3	Left-M	F	Left-M	Stop	Off	Off
4	Left-F	F	Left-Ft	Stop	Off	Off
5	Right-N	F	Right-Sl	Stop	Off	Off
6	Right-M	F	Right-M	Stop	Off	Off
7	Right-F	F	Right-Ft	Stop	Off	Off
8	Up-N	F	Stop	Up-Sl	Off	Off
9	Up-M	F	Stop	Up-M	Off	Off
10	Up-F	F	Stop	Up-Ft	Off	Off
11	Down-N	F	Stop	Down-Sl	Off	Off
12	Down-M	F	Stop	Down-M	Off	Off
13	Middle	F	Stop	Stop	Off	Off
14	Middle	N	Stop	Stop	On	On

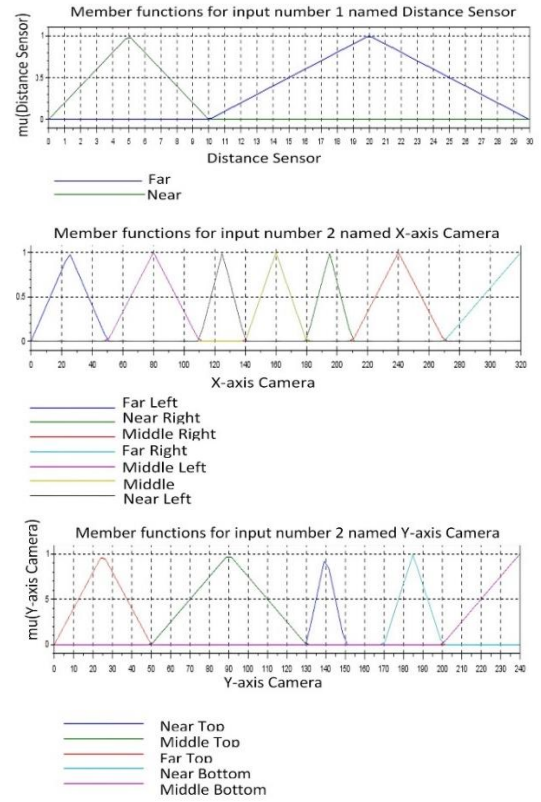

(a) Membership function of input

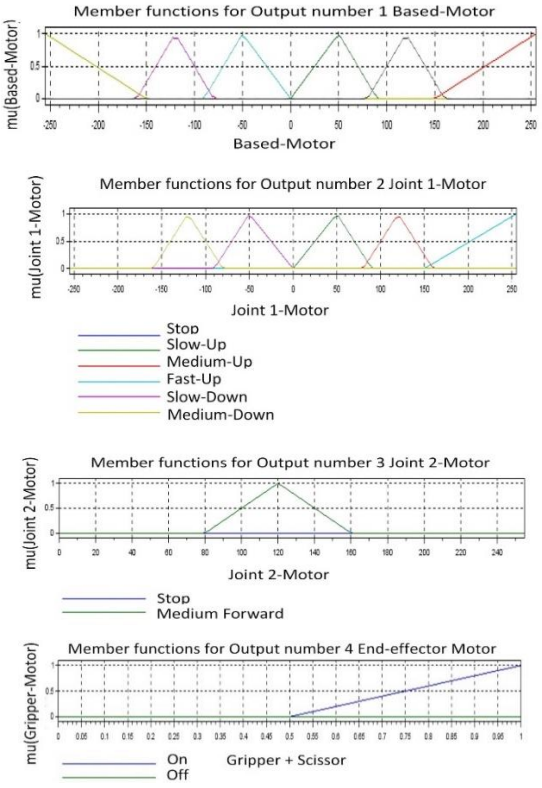

(b) Membership function of output

Figure 5. The membership function of input and output is considered in this study.

The membership function considered in this study is given by

$$A(x) = \begin{cases} 0, & x < 0 \\ \frac{x-a}{m-a}, & x \geq 0 \\ \frac{b-x}{b-m}, & x \geq 0 \\ 0, & x \geq 0 \end{cases}, \quad (12)$$

where a, m, and b are based on x and y -positions achieved online during the task.

RESULTS AND DISCUSSION

Experiments are undertaken to validate the efficacy of the proposed visual servoing method coupled with Fuzzy Logic Control (FLC) by deploying the robot for strawberry harvesting with the experimental setup depicted in Figure 6.

The robot is set to cut (using scissors) and grab (using a gripper) 3 strawberries marked as left, middle, and right, one at a time. The robot can work for 3 hours without stopping, supported by a 2200 mAh battery. The experiment was conducted 120 times, 60 times without FLC, and 60 times with FLC. 60 times are divided into 20 times for harvesting the middle, 20 times for the left side, and 20 times for the right-side strawberry.

The robot is activated as the camera detects the position of the strawberries. The microcontroller moves the joints and end-effector accordingly. The end-effector consists of scissors to cut the strawberry and a gripper to grab it, and the motor servo in the base moves the robot to put the strawberry inside the prepared basket, as shown in Figure 6. The considered image plane in this study has a resolution of 320×240 pixels within the speed of 30fps; therefore, $the\ x$-axis starts from $0 - 320$ pixels, and $the\ y$-axis is $0 - 240$ pixels.

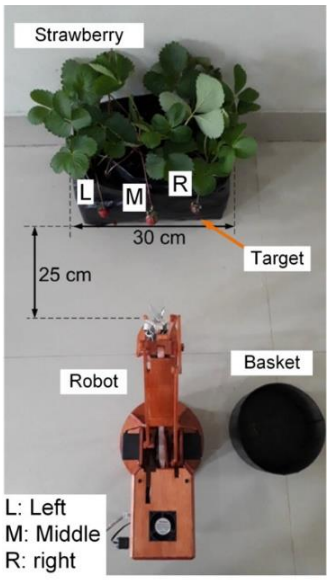

Figure 6. Experimental Setup

Table 3 outlines the relationship between strawberry detection, its position in the image plane, and the robot's motion relative to the end-effector. The x-coordinate represents the target position, while the y-coordinate indicates its location in the image plane.

Figure 7 is strawberry detection using image segmentation where the target position in x and y coordinates becomes the input to the microcontroller to control the end-effector's direction and speed in reaching the target before cutting and gripping it, as shown in Table 3. The process of picking the object starts with the strawberry located in the middle of the image place since it is the closest one to the robot.

Figure 8 illustrates the multiple image segmentation procedures carried out in this research. The identified strawberry with greater prominence is considered closer to the end-effector, while smaller targets are positioned on either side of the image plane. Figure 9 shows the robot harvesting a centrally positioned strawberry, identified as the most prominent object. Image segmentation proved more robust against varying lighting, demonstrating the method's effectiveness.

Table 3. The relationship between target position and end-effector motion

x and y axis Position	Target Position	End-effector Motion
$x \geq 140$ & $x \leq 180$ & $y \geq 150$ & $x \leq 170$	Middle	Forward
$x > 110$ & $x < 140$	Left-Near	Left-Slow
$x > 50$ & $x \leq 110$	Left-Medium	Left-Medium
$x \leq 50$	Left-Far	Left-Fast
$x > 180$ & $x \leq 210$	Right-Near	Right-Slow
$x > 210$ & $x < 270$	Right-Medium	Right-Medium
$x \geq 270$	Right-Far	Right-Fast

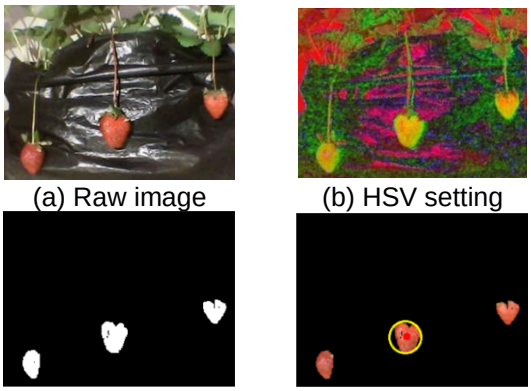

(a) Raw image (b) HSV setting

(c) Thresholding processed (d) The closest detected strawberry

Figure 7. Image segmentation process for strawberry detection in this study

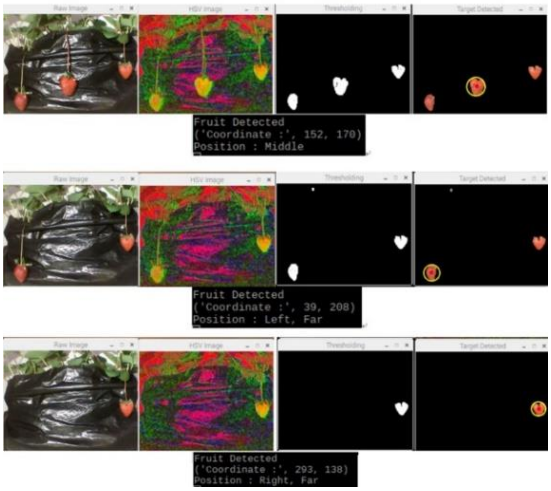

Figure 8. Various strawberries are detected during harvesting, starting from the closest one.

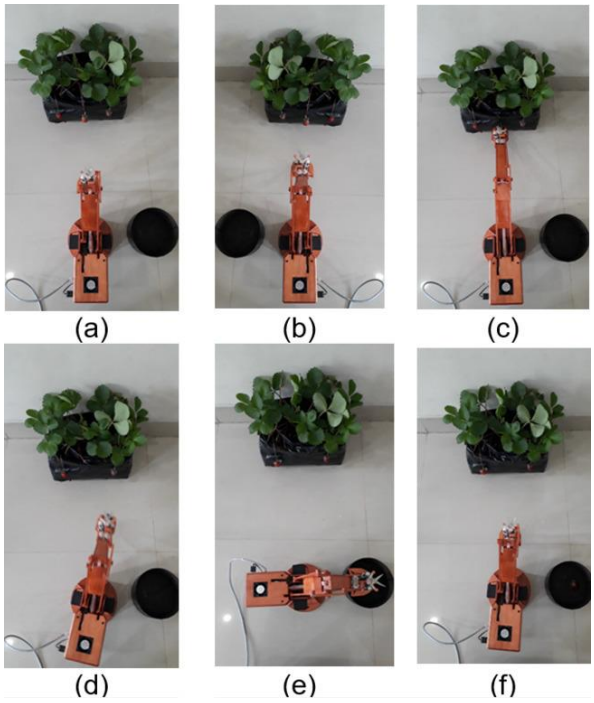

Figure 9. Strawberry picking process when the detected strawberry is located in the middle of the image plane

The harvesting experiment was repeated 20 times per criterion, with results detailed in Table 4. The findings also highlight better performance with FLC compared to without it.

Table 4 compares the robot's hit rate with and without FLC, where "O" signifies a "hit" and "✕" a "miss." In both setups, the robot primarily picks the closest strawberry, typically the middle one due to its central position. As a result, the middle strawberry shows higher hit rates (80% without FLC and 95% with FLC). The increase in hits with FLC highlights its effectiveness.

Table 4. The hit rate comparison

nth-Experiment	Target Position					
	Without FLC			With FLC		
	L	M	R	L	M	R
1	✕	O	O	O	O	O
2	✕	O	✕	O	O	O
3	✕	O	O	O	O	O
4	✕	✕	✕	O	✕	O
5	✕	O	✕	O	O	O
6	O	✕	O	✕	O	O
7	✕	O	✕	✕	O	O
8	O	O	✕	✕	O	O
9	O	O	O	O	O	O
10	✕	O	O	O	O	O
11	✕	O	O	O	O	O
12	O	O	O	O	O	✕
13	O	O	✕	O	O	O
14	O	O	O	O	O	✕
15	O	O	✕	O	O	O
16	O	✕	O	O	O	✕
17	O	O	✕	O	O	O
18	O	O	O	O	O	O
19	✕	O	✕	✕	O	O
20	O	✕	O	O	O	✕
Total	11	16	11	16	19	16
% Hit rate	55%	80%	55%	80%	95%	80%
Overall	38 or 63%			51 or 85%		

Table 5. Time comparison in completing the task.

Pose	nth-Exp.	Without FLC (s)			With FLC (s)		
		T_1	T_2	T_3	T_1	T_2	T_3
Left	1	6.5	8.8	10.4	8.5	10.9	12.4
	2	7.5	9.7	11.3	9.4	11.7	13.3
	3	7.7	10.1	11.8	8.4	10.7	12.2
	4	6.8	9.3	10.9	9.0	11.3	13.0
	5	6.7	8.9	10.5	9.3	11.8	13.4
	Av.	**7.0**	**9.4**	**11.0**	**8.9**	**11.3**	**12.9**
Middle	1	9.3	11.4	13.1	7.1	9.5	11.1
	2	9.3	12.0	13.6	9.0	11.5	13.6
	3	10.1	12.7	14.3	7.4	9.9	11.4
	4	9.5	11.8	13.3	7.4	9.7	11.2
	5	9.0	11.5	12.9	7.1	9.79	11.1
	Av.	**9.4**	**11.9**	**13.5**	**7.6**	**10.1**	**11.7**
Right	1	9.5	11.8	13.3	6.7	8.9	10.5
	2	16.0	18.3	19.8	7.3	9.6	11.0
	3	19.6	21.8	23.3	7.1	9.5	10.8
	4	10.6	12.8	14.3	7.1	9.4	10.9
	5	11.7	13.9	15.4	7.4	9.8	11.2
	Av.	**13.5**	**15.7**	**17.2**	**7.1**	**9.4**	**10.9**

Without FLC, the robot achieved 11 hits (L), 16 hits (M), and 11 hits (R), with hit rates of 55%, 80%, and 55%, respectively, leading to a 63% overall rate. With FLC, hits improved to 16 (L), 19 (M), and 16 (R), with hit rates of 80%, 95%, and 80%, raising the overall rate to 85%. Table 4 underscores the significant improvement with FLC, particularly for the middle target, increasing the overall success rate from 63% to 85%.

The time required for the robot to accomplish its task of harvesting strawberries is presented in Table 5. T_1 is the time needed from

detection to the target-cutting process, T_2 is the time from detection, target-cutting, and placing the target in the basket, and T_3 is the time from completing the task and returning to the initial position. The most significant improvement of FLC implementation is observed in the Right pose, with times nearly halved, as the robot refers to rules-based, as stated in Table 2.

The experimental results show that the combination of image segmentation for image processing and FLC for processing object detection inputs significantly improves the robot's performance without requiring sophisticated resources; hence, the proposed method can be applied in agriculture because it is user-friendly for any farmer.

CONCLUSION

This paper introduces an FLC design and image segmentation approach for a strawberry harvesting robot. The robot is tasked with cutting, grabbing, and placing strawberries into a basket. The image segmentation process is designed to require minimal computational power, making it suitable for use on a Raspberry Pi, which has limited memory but can effectively handle the task. The mechanical and electrical designs of the robot are also simplified, allowing farmers to build and use it for harvesting seasonal fruit. FLC is employed to enhance the robot's performance, resulting in a higher hit rate and faster harvesting times. In 60 experiments without FLC, the robot achieved an 80% hit rate for strawberries positioned in the middle of the image plane and 55% for those on the left and right. In contrast, with FLC, the hit rate improved to 95% for the middle and 80% for the left and right positions. The average task completion time without FLC was 13.51 seconds for strawberries in the middle, 11.04 seconds for the left, and 17.28 seconds for the right. With FLC, the times improved to 12.90 seconds for the middle, 11.71 seconds for the left, and 10.93 seconds for the right. The reduced harvesting time allows for more strawberries to be picked daily, increasing overall production. The proposed method has demonstrated its effectiveness in controlling the strawberry harvesting robot, which has practical applications in agriculture. Future work will focus on designing a more practical and reproducible robot.

ACKNOWLEDGMENT

The authors would like to thank Politeknik Negeri Sriwijaya for the funding and the supporting academic atmosphere.

REFERENCES

[1] Y. Oktarina, Z. Nawawi, B. Y. Suprapto and T. Dewi, "Digitized Smart Solar Powered Agriculture Implementation in Palembang, South Sumatra," *2023 10th International Conference on Electrical Engineering, Computer Science and Informatics (EECSI)*, Palembang, Indonesia, 2023, pp. 60-65, doi: 10.1109/EECSI59885.2023.10295805.

[2] Y. Oktarina, Z. Nawawi, B. Y. Suprapto and T. Dewi, "Solar Powered Greenhouse for Smart Agriculture," *2023 International Conference on Electrical and Information Technology (IEIT)*, Malang, Indonesia, 2023, pp. 36-42, doi: 10.1109/IEIT59852.2023.10335599.

[3] D. T. Fasiolo, L. Scalera, E. Maset, and A. Gasparetto, "Towards autonomous mapping in agriculture: A review of supportive technologies for ground robotics," *Robotics and Autonomous Systems*, vol. 169, 104514, 2023, doi: 10.1016/j.robot.2023.104514.

[4] M. Wakchaure, B.K. Patle, and A.K. Mahindrakar, "Application of AI techniques and robotics in agriculture: A review," *Artificial Intelligence in the Life Sciences*, vol. 3, 100057, 2023, doi: 10.1016/j.ailsci.2023.100057.

[5] J. Cox, N. Tsagkopoulos, Z. Rozsypálek, T. Krajník, E. Sklar, and M. Hanheide, "Visual teach and generalise (VTAG)—Exploiting perceptual aliasing for scalable autonomous robotic navigation in horticultural environments," *Computers and Electronics in Agriculture*, vol. 212, 108054, 2023, doi: 10.1016/j.compag.2023.108054.

[6] Y. Mases, T. Dewi and Rusdianasari, "Solar Radiation Effect on Solar Powered Pump Performance of an Automatic Sprinkler System," *2021 International Conference on Electrical and Information Technology (IEIT)*, Malang, Indonesia, 2021, pp. 246-250, doi: 10.1109/IEIT53149.2021.9587360.

[7] E. V. Novaldo, T. Dewi and Rusdianasari, "Solar Energy as an Alternative Energy Source in Hydroponic Agriculture: A Pilot Study," *2022 International Conference on Electrical and Information Technology (IEIT)*, Malang, Indonesia, 2022, pp. 202-205, doi: 10.1109/IEIT56384.2022.9967806.

[8] D. A. Nugraha, T. Dewi and Y. Bow, "The Concept of Energy Generation by Solar Panel and Pico Hydro in Household Application," *2023 International Conference on Electrical and Information Technology (IEIT)*, Malang, Indonesia, 2023, pp. 31-35, doi: 10.1109/IEIT59852.2023.10335531.

[9] M. H. Dairath, M. W. Akram, M. A. Mehmood, H. U. Sarwar, M. Z. Akram, M. M. Omar, M. Faheem, "Computer vision-based prototype robotic picking cum grading system for fruits," *Smart Agricultural Technology*, vol. 4, 100210, 2023, doi: 10.1016/j.atech. 2023.100210.

[10] G. Hu, C. Chen, J. Chen, L. Sun, A. Sugirbay, Y. Chen, H. Jin, S. Zhang, and L. Bu, "Simplified 4-DOF manipulator for rapid robotic apple harvesting," *Computers and Electronics in Agriculture*, vol. 199, 107177, 2022, doi: 10.1016/j.compag.2022.107177.

[11] T. Dewi., S. Nurmaini., P. Risma, and Y. Oktarina, "Inverse Kinematic Analysis of 4 DOF Pick and Place Arm Robot Manipulator using Fuzzy Logic Controller," *International Journal of Electrical and Computer Engineering (IJECE)*, vol. 10, no. 2, pp. 1376-1386, 2020, doi: 10.11591/ijece.v10i2. pp1376-138

[12] A. Al-Shanoon and H. Lang, "Robotic manipulation based on 3-D visual servoing and deep neural networks," *Robotics and Autonomous Systems*, vol. 152, 104041, 2022, doi: 10.1016/j.robot.2022.104041.

[13] Y. Yang, Y. Han, S. Li, Y. Yang, M. Zhang, H. Li, "Vision based fruit recognition and positioning technology for harvesting robots," *Computers and Electronics in Agriculture*, vol. 213, 108258, 2023, doi: 10.1016/j.compag.2023.108258.

[14] Y. Park, C. Kim, and H. I. Son, "Fast and stable pedicel detection for robust visual servoing to harvest shaking fruits," *Computers and Electronics in Agriculture*, vol. 220, 108863, 2024, doi: 10.1016/j.compag.2024.108863.

[15] T. Kim, D. Lee, K. Kim, and Y. Kim, "2D pose estimation of multiple tomato fruit-bearing systems for robotic harvesting," *Computers and Electronics in Agriculture*, vol. 211, 108004, 2023, doi: 10.1016/j.compag.2023. 108004.

[16] E. Kok, and C. Chen, "Occluded apples orientation estimator based on deep learning model for robotic harvesting," *Computers and Electronics in Agriculture*, vol. 219, 108781, 2024, doi: 10.1016/j.compag.2024.108781.

[17] T. Dewi., P. Risma., and Y. Oktarina, "Fruit Sorting Robot based on Color and Size for an Agricultural Product Packaging System," *Bulletin of Electrical Engineering, and Informatics (BEEI)*, vol. 9, no. 4, pp. 1438-1445, 2020. doi: 10.11591/eei.v9i4.2353.

[18] A. Al-Shanoon, and H. Lang, "Robotic manipulation based on 3-D visual servoing and deep neural networks," *Robotics and Autonomous Systems*, vol. 152, pp. 104041, 2022, doi: 10.1016/j.robot.2022.104041.

[19] Y. He, J. Gao, and Y. Chen, "Deep learning-based pose prediction for visual servoing of robotic manipulators using image similarity," *Neurocomputing*, vol. 491, pp. 343-352, 2022, doi: 10.1016/j.neucom.2022.03.045.

[20] A. Jokić, M. Petrović, Z. Miljković, "Semantic segmentation based stereo visual servoing of nonholonomic mobile robot in intelligent manufacturing environment," *Expert Systems with Applications*, vol. 190, 116203, 2022, doi: 10.1016/j.eswa.2021.116203

[21] J. Liang, K. Huang, H. Lei, Z. Zhong, Y. Cai, and Z. Jiao, "Occlusion-aware fruit segmentation in complex natural environments under shape prior," *Computers and Electronics in Agriculture*, vol. 217, 108620, 2024, doi: 10.1016/j.compag.2024. 108620.

[22] T. Dewi., P. Risma., Y. Oktarina., and S. Muslimin, "Visual Servoing Design and Control for Agriculture Robot; a Review," *Proc. 2019 ICECOS*, 2-4 Oct. 2018, Pangkal Pinang: Indonesia, pp. 57-62, 2018, doi: 10.1109/ICECOS.2018.8605209.

[23] T. Dewi, P. Risma., and Y. Oktarina, "Fuzzy Logic Simulation as Teaching-Learning Media for Artificial Intelligence Class, Journal of Automation," *Mobile Robotics & Intelligent Systems*, vol. 12, no. 3, pp. 59-65, 2018, 10.14313/jamris_3-2018/13.

[24] H. Xu, H. Chen, M. A.H. Ali, W. Liu, and Z. Wang, "Anti-windup uniform fuzzy control for uncertain wheeled mobile robots," *Journal of the Franklin Institute*, ID: 106807, 2024, doi: 10.1016/j.jfranklin.2024.106807.

[25] Y. Shen, "Robotic trajectory tracking control system based on fuzzy neural network," *Measurement: Sensors*, vol. 31, ID: 101006, 2024, doi: 10.1016/j.measen.2023.101006.

[26] D. Romahadi, D. Feriyanto, F. Anggara, F. P. Wijaya, W. Dong, "Intelligent system design for identification of unbalance and misalignment using Fuzzy Logic methods," *SINERGI*, vol. 28, no. 2, pp. 241-250, 2024, doi: 10.22441/sinergi.2024.2.004

[27] H. Suwoyo, M. H. I. Hajar, P. Indriyanti, A. Febriandirza, "The use of Fuzzy Logic Controller and Artificial Bee Colony for optimizing adaptive SVSF in robot localization algorithm," *SINERGI*, vol. 28, no. 2, pp. 231-240, 2024, doi: 10.22441/sinergi. 2024.2.003